Aerosol and Air Quality Research, 18: 3009–3024, 2018
Copyright © Taiwan Association for Aerosol Research
ISSN: 1680-8584 print / 2071-1409 online
doi: 10.4209/aaqr.2017.11.0508

Contribution of Regional Transport to Surface Ozone at an Island Site of Eastern China

Lei Tong[1,2+], Jingjing Zhang[1,2,3+], Honghui Xu[4], Hang Xiao[1,2*], Mengmeng He[1,2], Huiling Zhang[5]

[1] *Center for Excellence in Regional Atmospheric Environment, Institute of Urban Environment, Chinese Academy of Sciences, Xiamen 361021, China*
[2] *Key Lab of Urban Environmental Processes and Pollution Control, Ningbo Urban Environment Observation and Research Station-NUEORS, Chinese Academy of Sciences, Ningbo 315830, China*
[3] *University of Chinese Academy of Sciences, Beijing 100409, China*
[4] *Zhejiang Institute of Meteorological Sciences, Hangzhou 310008, China*
[5] *Ningbo Urban Planning and Geographic Information Center, Ningbo 315042, China*

ABSTRACT

The surface ozone (O_3) in non-urban areas can be strongly influenced by transported regional air pollutants from distant urban agglomerations. Comprehensively using the polar plot graphical technique, and backward trajectory and potential source contribution analyses, the variations of surface O_3 and its potential source regions at an island site of Zhejiang, China, were analyzed based on data from June 2013 to October 2016. Relatively high hourly O_3 levels (max.: 154.0 ppb) were often observed, with the total number of hourly O_3 exceeding the national standard (75 ppb) being 583, indicating high health risks from O_3 exposure. An obvious time-lag for the diurnal O_3 peak was observed, with the daily maxima often occurring at 16:00. A decreased O_3 level was observed in summer, which was probably due to the comprehensive influence of intense rainfall, high relative humidity and clean marine airmasses during this season. The transport of external air pollutants played a dominant role in affecting local O_3, with relatively high O_3 concentrations (> 50 ppb) being observed under high wind speeds (> 5 m s^{-1}). Based on all the source identification analyses, the major regions contributing to the surface O_3 lay to the north and northwest of the study area. Long-range transported air pollutants from the coastal provinces of the North China Plain may have significantly enhanced surface O_3 at the study site, while contributions from local areas and areas to the south of the study site were rather small. A high incidence (64.3%) of O_3 pollution was accounted for by the inflowing airmasses from outside of Zhejiang, which quantitatively confirmed the significant background transport of O_3 to this province. Coordinated inter-regional control on pollutant emissions should be carried out to reduce O_3 in Zhejiang Province.

Keywords: Backward trajectories; Potential source contribution function (PSCF); Polarplot; O_3 inflow.

INTRODUCTION

Surface ozone is a major trace gas which is of great importance for climate and air quality. It is mainly produced from its precursors such as carbon monoxide (CO), non-methane volatile organic compounds (NMVOCs) and nitrogen oxides (NO_x) by photochemical reactions in the presence of sufficient solar radiation (Sillman, 1999). High levels of O_3 can adversely affect vegetation growth and human health due to its strong oxidizability and phytotoxicity (Monks *et al.*, 2015). A large quantity of crop yield loss and premature human deaths have been reported to be O_3-related (Fann *et al.*, 2012; Feng *et al.*, 2015). Besides, as the third major greenhouse gas, O_3 could play an important role in the process of global warming (Stocker *et al.*, 2013).

With the increasing anthropogenic emissions of O_3 precursors, a steady rise in ground-level O_3 was widely observed or predicted (Nopmongcol *et al.*, 2016), especially in the mid-latitude regions of northern hemisphere where background O_3 concentrations have increased continuously (0.5–2% per year) during past decades (Vingarzan, 2004). As the biggest developing country in the world, China has experienced tremendous changes in recent years. Continuous rapid urbanization and industrialization in China has made it a photochemically polluted region, with rising concentrations of O_3 and its precursors being a matter of growing concern

[+] The two authors contributed equally to this paper.

[*] Corresponding author.
Tel.: 86-574-8678-4813; Fax: 86-574-8678-4813
E-mail address: hxiao@iue.ac.cn

for both public administrations and citizens (Ou *et al.*, 2016). High levels of O_3 exceeding the National Ambient Air Quality Standard (NAAQS) of China have been frequently observed in developed urban areas (Li *et al.*, 2016a; Tong *et al.*, 2017a).

Given the damaging effects of surface O_3 on populations and ecosystems, and the increasing trends of its concentrations, it is critical to identify the possible sources of O_3, which is fundamental to design effective strategies on emission controls. Surface O_3 has three major sources, i.e., *in situ* photochemical production, lateral boundary import, and downward transport from upper atmosphere (e.g., stratosphere) (Ma *et al.*, 2002; Lin *et al.*, 2015; Zhu *et al.*, 2016). Due to the influences of meteorological conditions and the nonlinear relationships between O_3 and its precursors, it is usually complicated to accurately identify the sources of O_3 at a specific location. Over the past several decades, great efforts have been made on this subject by researchers worldwide. For example, using a regional three-dimensional chemical transport model (3-D CTM), Berntsen *et al.* (1999) studied the transport of O_3 across the North Pacific and evaluated the influence of Asian emissions on the air quality of the United States; Ma *et al.* (2002) analyzed the contributions of various sources to the O_3 distributions in the troposphere over China during summertime based on a global 3-D CTM; Sudo and Akimoto (2007) quantified the contributions from different source regions to global distributions and budgets of tropospheric O_3 in the context of intercontinental transport using the tagged tracer simulation; Demuzere *et al.* (2009) and Pope *et al.* (2016) assessed the influences of the large-scale circulation on O_3 in the Netherlands and the United Kingdom, respectively, using the objective Lamb weather type approach; Shen *et al.* (2015) quantified the sensitivity of O_3 air quality in the eastern United States to the major patterns in synoptic-scale circulation by applying empirical orthogonal functions; Li *et al.* (2016b) estimated the cross-boundary transport of O_3 between Beijing and the North China Plain by applying comprehensively the bivariate polar plot graphical technique, the transport flux assessment and the potential source contribution function (PSCF) analysis. All these previous studies have provided important insights into the causes and control strategies of O_3 pollution. However, a majority of them were carried out in urban areas but few in suburban and rural areas, where the O_3 levels might be even higher due to the contributions of O_3 precursors from regional transport (Chiang *et al.*, 2009; Kanaya *et al.*, 2016).

Zhoushan is a small island city of Zhejiang Province in eastern China. The level of industrialization in the city is low with less emission of primary air pollutants into the atmosphere. Due to the influences of subtropical monsoon and strong sea-land breezes, local formation and accumulation of secondary air pollutants are also weak. Consequently, Zhoushan has been continuously one of the top ten cities with the best air quality in China in recent years (http://datacenter.mep.gov.cn/index). In contrast, the area near Zhoushan, i.e., the Yangtze River Delta (YRD) region, is more polluted with substantial air pollutants being emitted annually (Fu *et al.*, 2013). YRD is one of the most developed and heavily-polluted city clusters of China, which consists of Shanghai Municipality and another 25 cities within Jiangsu, Zhejiang and Anhui Provinces (Fig. S1). The annual emissions of NO_x and NMVOCs in the YRD region are estimated to be 2776 and 3822 kiloton, respectively, in 2010, and the VOC emissions increased by 110% from 2000 to 2010 (Fu *et al.*, 2013). The majority of these air pollutants are accounted for by industrial and traffic emissions from large cities such as Shanghai and Suzhou (Fu *et al.*, 2013). The significant differences in the pollution statuses between Zhoushan and its surrounding cities create a good condition for the study of regional influences on local air quality.

So far, no published studies about surface O_3 in the city of Zhoushan have been reported, although high levels of O_3 over the NAAQS were frequently observed during warm seasons (http://datacenter.mep.gov.cn/index). In this study, the O_3 pollution in Zhoushan over the period of June 2013–October 2016 was analyzed based on different techniques, including the bivariate polar plot graphical technique, the backward trajectory analysis, the potential source contribution function (PSCF) analysis, and case studies under shifting wind conditions. The main objectives are to determine the potential regions contributing to surface O_3 in Zhoushan, and to assess the influence of regional transport on O_3 pollution in this island city of eastern China.

METHODS

Study Area

Zhoushan is one of the most important port cities for opening to the outside world of China. This city is famous for its developed marine fishery and port transportation. Zhoushan has the biggest fishing ground of China, and it is also a major component of Ningbo-Zhoushan port, which is the largest container port in the world with annual cargo throughput being higher than 900 million tons in 2016. As to the topography of Zhoushan, it is mountainous and about 70% of its land is covered by hills with altitudes of 200–300 m. The study site is located in the Administrative Service Center of Putuo District (ACPD) (29°57′N, 122°19′E), which is in the southeast of the city of Zhoushan (Fig. 1). This site is in a comprehensive area with a few commercial and residential buildings nearby. A mountain is 0.2 km away from the west of ACPD while the sea is 0.8 km away from the east of this site. Some small islands with relatively developed tourism are distributed along the southeast to the study site.

In terms of the climate conditions, the study area is subject to the sub-tropical monsoon with hot, humid summers and cool, damp winters. The annual mean air temperature (T), relative humidity (RH) and precipitation are 16.7°C, 79% and 1222.6 mm, respectively. The air temperature reaches its maximum (25.8–28.0°C) and minimum (5.2–5.9°C) in August and January, respectively. Intensive precipitation often occurs in June and August due to the influences of plum rain and typhoon weather. Annual mean wind speed is 3.5 m s^{-1} with northwest and southeast winds being dominant in winter and summer, respectively.

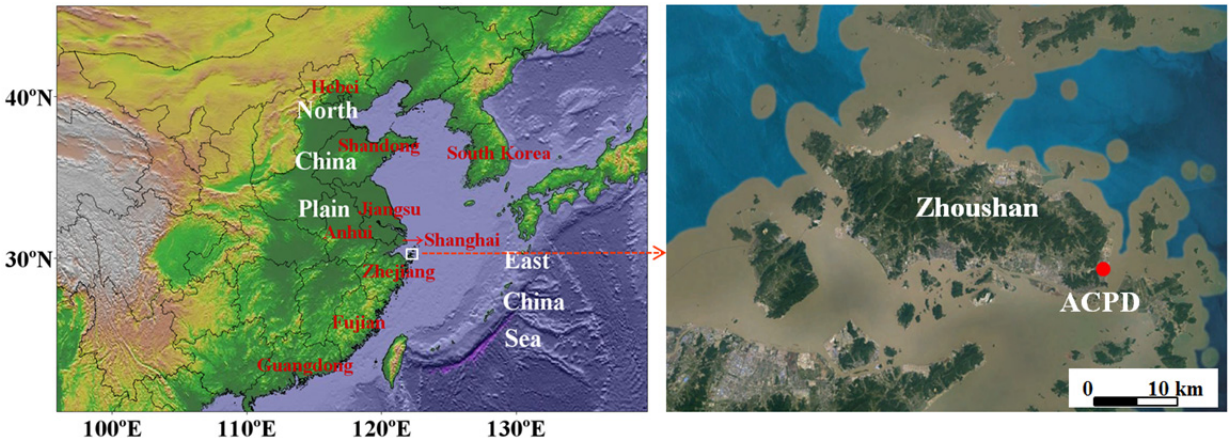

Fig. 1. Map of the sampling site of Administrative Service Center of Putuo District (ACPD) in Zhoushan, China.

Data Collection

In-situ measurements of surface O_3 were carried out with a commercial trace gas instrument (Model 49i, Thermo Fisher Scientific Inc., USA). It functions on the absorption of ultraviolet light at 254 nm with the O_3 concentration being determined based on Lambert-Beer's law (Thermo Fisher Scientific Inc., 2017). Hourly average data monitored during the O_3 seasons (April–October) from June 2013 to October 2016 were used for analyses in this study. All times used are local time (China Standard Time, CST), which is 8 h ahead of the Coordinated Universal Time (UTC+8). In order to assess the influence of regional transport on surface O_3 in the study area, the hourly O_3 concentrations in the upwind cities of Jiangsu, Zhejiang and Fujian Provinces (Fig. S2) were collected from the data center of the National Ministry of Environmental Protection of China (MEPC) (http://datacenter.mep.gov.cn/). All the data released by MEPC were measured *in-situ* using commercial trace gas instruments (e.g., Model 49i, Thermo Fisher Scientific Inc., USA), which were maintained by third-parties to ensure the data quality. Meteorological data were also monitored on hourly basis using a portable automatic weather station (WS500-UMB, Lufft, Germany) established at ACPD. The meteorological variables applied in this study include air temperature (T, °C), relative humidity (RH, %), wind speed (WS, m s^{-1}), wind direction (WD, °) and rainfall (mm). For all the monitoring data, only the days with a minimum capture rate on hourly data of 75% and the months with at least 20 days of valid data were applied to statistical analyses.

Transport Direction Analysis

The relationships between pollutant concentrations and wind conditions can provide useful information on the transport directions of air pollutants. For example, high concentrations of air pollutants associated with high wind speeds often indicate significant regional contribution from upwind areas (Grange *et al.*, 2016). The transport directions of O_3 were analyzed in this study based on the bivariate polar plot graphical technique developed by Carslaw *et al.* (2006). Specifically, wind speed, wind direction and concentration data are partitioned into wind speed-direction bins with the mean concentrations being calculated for each bin. Then the wind components (u and v) are calculated with a generalized additive model (GAM) (Eq. (1)) being used to fit the surface data and to extract the possible source features:

$$\sqrt{C_i} = s(u_i, v_i) + e_i \quad (1)$$

where C_i is the calculated pollutant concentration, $s(u_i, v_i)$ is the isotropic smooth function of i^{th} value of covariate u and v, and e_i is the residual. Based on Eq. (1), a smoothed surface is fitted to the wind speed-direction bins to create a continuous surface which can be plotted with polar coordinates. More details about this equation can be found in Yu *et al.* (2004), Carslaw *et al.* (2006) and Grange *et al.* (2016). All the analyses were made with *Openair*, an R package for air quality data analysis (http://www.openair-project.org/Downloads/OpenAirManual.aspx).

Back Trajectory and PSCF Analyses

The backward trajectories of airmasses arriving at the study site were calculated using the HYSPLIT-4 model from the National Oceanic and Atmospheric Administration Air Resources Laboratory (http://ready.arl.noaa.gov/HYSPLIT.php) and the meteorological data from the National Centers for Environmental Prediction Global Data Assimilation System (1 × 1°) (ftp://arlftp.arlhq.noaa.gov/pub/archives/gdas1). A tracking time of 72 h was used in this study with hourly trajectories at 50, 500 and 1000 m above ground level (AGL) being calculated from 00:00 to 23:00 (UTC) during the O_3 seasons (April–June for 2013–2016). A total of 57,240 hourly trajectories (19,080 for each height) were calculated, which were mainly used for the following analyses: (1) All the 57,240 hourly trajectories were applied to the PSCF analysis to determine the potential regions contributing to surface O_3 at ACPD; (2) 1249 hourly trajectories with the arriving time at ACPD of 14:00 CST (June 2013–October 2016), when the O_3 concentrations were usually high enough to pose threats to human health under suitable photochemical conditions (e.g., high air temperature), were applied to determine the influence of

the inflowing airmasses to Zhejiang and (3) six hourly trajectories with the arriving time at ACPD of 14:00 CST were analyzed to further confirm the potential source regions of O_3 during the pollution episodes. As the trajectories with the starting height of 500 m AGL could represent the average flow field of atmospheric boundary layer (c.a. 1000 m AGL in height), in which air pollutants are well mixed by horizontal and vertical advections, only the 500-m trajectories were used for the (2) and (3) analyses above.

PSCF analysis, which is a useful tool for determining the potential source of a given chemical constituent (Ashbaugh *et al.*, 1985), was applied to identify the potential regions contributing to surface O_3 using the calculated trajectories of air parcels. The PSCF values can be regarded as the conditional probability that the concentrations of a given pollutant higher than the critical value are related to the passages of airmasses through a certain area during transport. It has been applied to identify the potential source regions of O_3 in different cities worldwide (e.g., Li *et al.*, 2016b; Vellingiri *et al.*, 2016).

In this study, the PSCF analysis was made using the Geographical Information System based software TrajStat (version 1.4.4R5), which is developed by Wang *et al.* (2009). The study domain for PSCF analysis was 2–75°N and 61–165°E with a resolution of 0.5 × 0.5°. The PSCF values could be calculated from the TrajStat software according to the equation as follow:

$$PSCF = M_{ij}/N_{ij} \quad (2)$$

where N_{ij} is the total number of trajectory endpoints in the ij^{th} grid cell and M_{ij} is the total number of trajectory endpoints in the same cell with the pollutant levels at the sampling site being greater than a criterion value (Ashbaugh *et al.*, 1985). The criterion value for O_3 was set at the 75th percentile of the dataset for the study period from June 2013 and October 2016. To reduce the uncertainty in cells with small N_{ij}, the PSCF values were multiplied by a weight function (W_{ij}), which was defined as follows (Wang *et al.*, 2015):

$$W_{ij} = \begin{cases} 1.00 & (80 < N_{ij}) \\ 0.70 & (25 < N_{ij} \le 80) \\ 0.42 & (15 < N_{ij} \le 25) \\ 0.17 & (N_{ij} \le 15) \end{cases} \quad (3)$$

Trajectory Analyses for the Air Flowing into Zhejiang

As Zhoushan is a border city in the northeast of Zhejiang Province (Fig. 1), the O_3 concentrations in the air parcels arriving at Zhoushan via East China Sea represent the background levels of O_3 flowing into Zhejiang Province. To assess the influences of background transport from outside of Zhejiang Province, afternoon (14:00 CST) 72-h back trajectories at ACPD over the study period were analyzed. According to Aleksic *et al.* (2016), only the trajectories, which spent less than three hours in Zhejiang Province before arriving at the study site, were used to eliminate the influence of pollutant emissions from within Zhejiang.

To explore the major pathways of airmasses flowing into Zhejiang, trajectories were clustered using TrajStat (version 1.4.4R5, http://www.meteothinker.com/downloads/index.html), which is a Geographical Information System (GIS)-based software developed by Wang *et al.* (2009). The clustering analysis was carried out based on Euclidean distances between trajectories, which were given by:

$$d_{12} = \sqrt{\sum_{i=1}^{n}((X_1(i) - X_2(i))^2 + ((Y_1(i) - Y_2(i))^2} \quad (4)$$

where X_1 (Y_1) and X_2 (Y_2) refer to backward trajectories 1 and 2, respectively. Initially, each trajectory is defined to be a cluster. For the first iteration, two trajectories are paired. For every combination of trajectory pairs, the cluster spatial variance, which is the sum of squared distance between the endpoints of cluster's component trajectories, is calculated. Then, the total spatial variance (TSV), the sum of all the cluster spatial variance, is calculated. The pair of clusters finally combined are the ones with the smallest change in TSV. The iterations continue until the last two clusters are combined. The percent change in TSV and number of clusters for each iteration are recorded. The final cluster number was determined by the point of inflexion on the curve of percent change in TSV vs. number of clusters (Fig. S3). More details about this methodology can be found in Draxler *et al.* (2014).

RESULTS AND DISCUSSION

Overview of Surface O_3

Relatively high O_3 levels over NAAQS (Grade I: 75 ppb; Grade II: 93 ppb) were often observed in Zhoushan during the study period (Fig. 2). For each O_3 season (April–October) of different sampling years, the number of hourly O_3 greater than Grade I NAAQS (75 ppb) varied from 37 in 2013 to 214 in 2015, with a total of 583 being observed during the whole study period (Table 1). The maximum O_3 concentration during the whole study period was as high as 154.0 ppb (May 28, 2014), which was 61 ppb higher than the Grade II NAAQS (93 ppb). All these results indicated the potential health risks of O_3 pollution to local people at the study site. Similar high O_3 concentrations ($\geq$ 150 ppb on hourly basis) were also observed in other cities (e.g., Hangzhou, Shanghai and Ningbo) of the same region (YRD) as this study (Xu *et al.*, 2008; Li *et al.*, 2016a; Tong *et al.*, 2017a). During warm seasons, the O_3 pollution could occur on the regional scale of eastern China (Wang *et al.*, 2006). In view of the harmful effects of O_3 on human health, effective measures on the emission control of O_3 precursors around the whole region are urgently needed.

In general, the monthly variation of O_3 showed an opposite trend with that of air temperature (Figs. 3 and 4), with a significant negative correlation (Spearman's rank

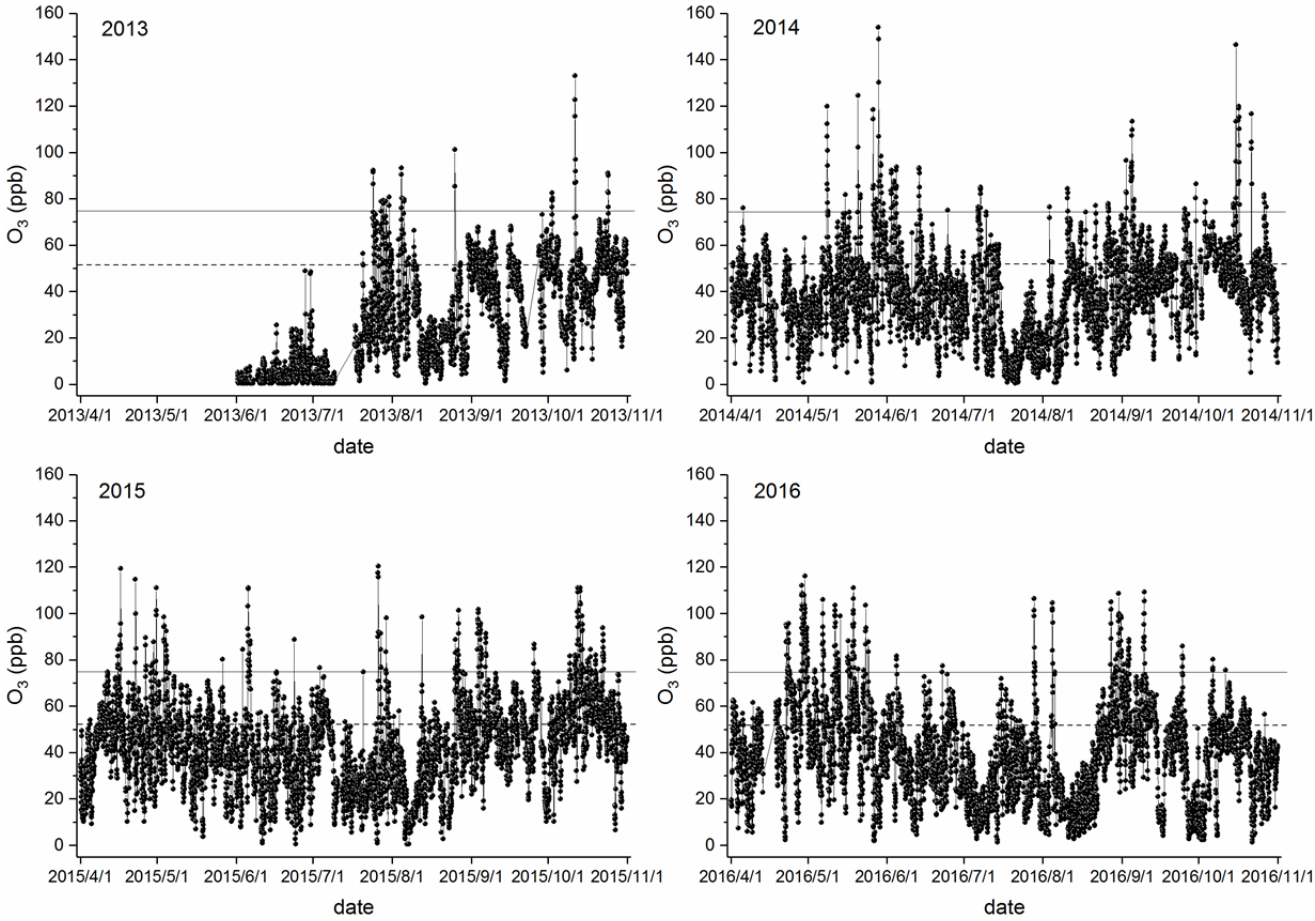

Fig. 2. Time series of hourly average O_3 concentrations at ACPD over the period of June 2013–October 2016. The horizontal solid and dash lines indicate the Grade I NAAQS (75 ppb), and the 75th percentile of the O_3 observations (51.8 ppb), respectively.

Table 1. Statistics of the O_3 observations during the study period.

Years	TN_{days} [a]	N_{days} [b]	N_{hours} [c]	Mean (ppb)	Median (ppb)	75th percentile (ppb)	Max. O_3 (ppb)	N_{days} > 75 ppb [d]	N_{hours} > 75 ppb [e]
2013	214	110	2415	30.4	30.7	47.1	133.0	11	37
2014	214	185	4178	39.8	41.6	50.9	154.0	33	137
2015	214	198	4511	42.8	43.4	54.1	120.4	42	195
2016	214	193	4557	39.1	38.9	51.8	116.2	35	214
2013–2016	856	686	15661	39.0	40.4	51.8	154.0	121	583

[a] TN_{days}: the total number of days for the O_3 seasons (April-October) of each year; [b] N_{days}: the number of days of the O_3 observations; [c] N_{hours}: the number of hours of the O_3 observations; [d] N_{days} > 75ppb: the number of days with the maximum hourly O_3 observations exceeding Grade I NAAQS (75 ppb); [e] N_{hours} > 75ppb: the number of hourly O_3 observations exceeding Grade I NAAQS (75 ppb).

correlation coefficient r = –0.26, p < 0.001) being observed between both variables for the whole study period. The O_3 levels were relatively high in spring (April and May) and autumn (September and October), and were obviously low in summer (June–August). This was contrary to the relatively high O_3 levels in summer, which have been widely observed worldwide (Dueñas *et al.*, 2004; Mavroidis and Ilia, 2012). The possible reasons for the summer minimum of O_3 observed at ACPD are as follows: (1) In this study, higher precipitation was observed in summer (Fig. 4), which indicated cloudy and rainy weather that are unfavorable to the photochemical generation of O_3. This might partly account for the low O_3 concentration observed during summertime. Similar effect of summer rainfall on surface O_3 has also been reported by Jo and Park (2005), Reddy *et al.* (2012) and Tong *et al.* (2017b). (2) The high relative humidity, which was observed simultaneously with the high air temperature in summer (Fig. 4), was favorable to the O_3 removal. As reported by Fiore *et al.* (2002), O_3 can be easily removed via reactions with water vapor under humid

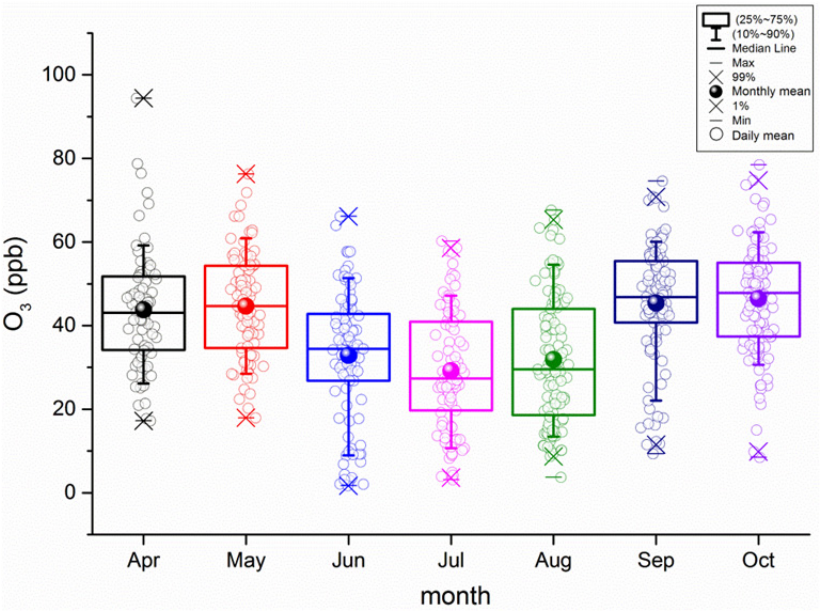

Fig. 3. Variations in monthly average O_3 concentrations (solid circles) and daily average O_3 concentrations by month (hollow circles) at ACPD over the period of June 2013–October 2016.

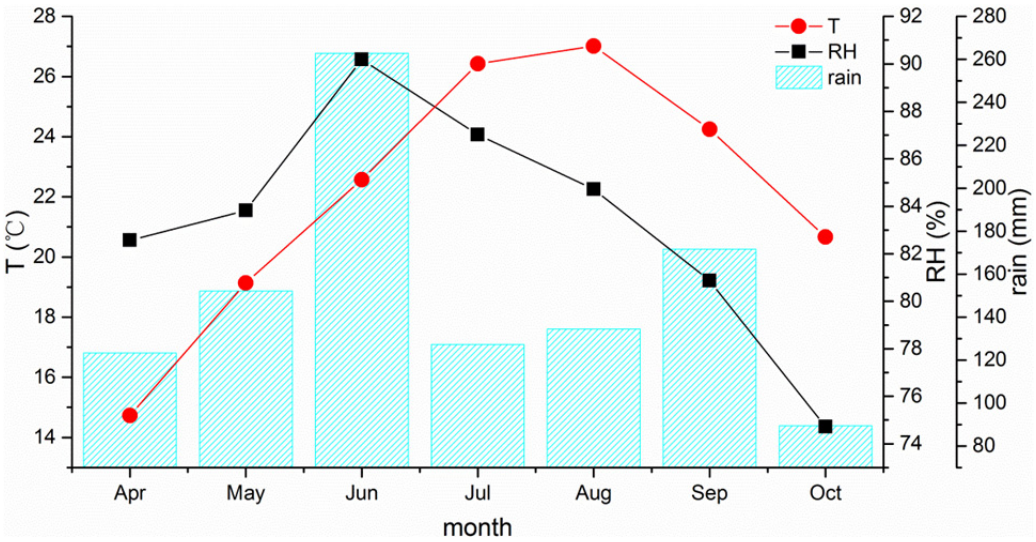

Fig. 4. Variations in monthly average air temperature, relative humidity and rainfall at ACPD over the period of June 2013–October 2016.

weather conditions. With the increase of relative humidity relating to greater cloud abundance, the photochemical processes associated with O_3 generation will be slowed down while O_3 depletions will be enhanced (Londhe *et al.*, 2008). This process of O_3 removal can be partly confirmed by the significant negative correlation between O_3 and RH ($r = –0.49$, $p < 0.001$) observed in this study. Therefore, the highest RH observed in summer at ACPD (Fig. 4) would probably contribute to the decrease in surface O_3. (3) The study site was predominantly influenced by summer monsoon from June to August, when most (66.3%) of the airmasses arriving at Zhoushan came from the east and south marine area during the study period. These clean airmasses with less O_3 and its precursors might play an important role in reducing local O_3 concentration at the study site. The cleaning effect of inflowing marine airmasses, which resulted in the summer minimum of O_3, has also been observed in other areas of East Asia (Zhang and Oanh, 2002).

As to the diurnal variation, hourly average O_3 concentration for the whole study period varied from 29.4 to 48.2 ppb (Fig. 5). The daily variation of O_3 concentration obviously lagged behind that of air temperature. The maximum value of O_3 occurred at 16:00, which is three hours later than the highest air temperature (13:00). Similar time lags for O_3 peaks were also observed in rural areas of other cities like Beijing and Hangzhou, China (Xu *et al.*, 2011; Li *et al.*, 2017). The possible reason for the O_3 time lag observed at ACPD might be the weak contribution from local sources

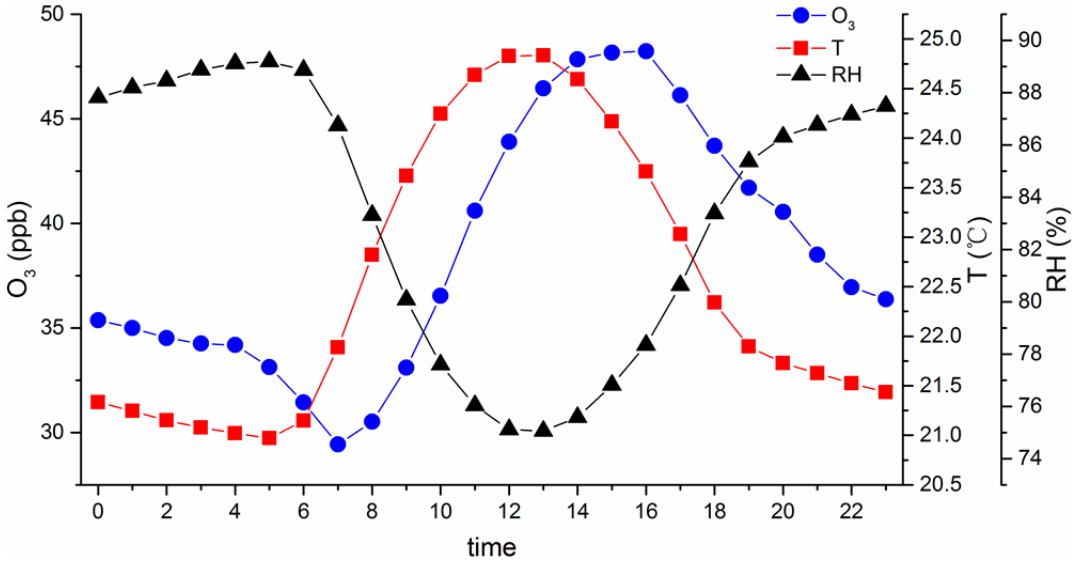

Fig. 5. Diurnal variations of average O_3 concentration, air temperature and relative humidity at ACPD over the period of June 2013–October 2016.

but relatively strong regional contribution to surface O_3 in the study area. As reported by Fu *et al.* (2013), a considerable amount of VOCs (131.0 kiloton), which is close to the median (134.1 kiloton) among the 25 cities in the YRD of China, were emitted annually in Zhoushan. However, the NO_x emission (13.3 kiloton) was the lowest of all the cities. The total emission amount of O_3 precursors (NO_x + VOCs) was smaller in Zhoushan than most of other cities in the YRD, which indicated less potential for O_3 production from precursors emitted locally. The ratio of NO_x to VOCs is an important factor in affecting O_3 formation (Sillman, 1999). Given the small emission amount of NO_x, the *in-situ* O_3 production might also be low under an NO_x-limited condition. Besides, the study site is located in a coastal area with relatively high wind speed of 3.9 m s^{-1} (diurnal average) during the study period. The *in-situ* photochemical production and accumulation of O_3 might be low as well, due to the cleaning effect of sea breeze. Therefore, the daily O_3 peak, which usually occurs at noon with the highest temperature, was inconspicuous due to the weak contribution from local emission sources. In comparison with the *in-situ* O_3 formation, the regional transport of air pollutants had played a more important role in the local O_3 increases (see the results from the PSCF and the Polarplot analyses in the latter part of the text). It may take longer time for the accumulation of surface O_3 to the maximum level after distant transport of air pollutants (Xu *et al.*, 2011), which might account for the peak lag of O_3 observed in this study.

Associations of O_3 with Wind Direction/Speed

Based on the polarplot analyses, high levels (> 50 ppb) of O_3 were found to be associated with airmasses coming from north and northwest areas to the study site (Fig. 6(a)). Local production of O_3 was relatively weak with lower O_3 levels when wind speed was close to zero. In contrast, long-range transport of air pollutants had significantly contributed to surface O_3 at the study site, which can be inferred from the high O_3 concentrations (> 50 ppb) occurring under high wind speeds (> 5 m s^{-1}) (Fig. 6(a)). These are similar to the results found in the coastal region of northeastern Iberian Peninsula, where high surface O_3 levels were not produced *in situ* but were largely contributed from horizontally advected flows (Gonçalves *et al.*, 2009). The north region to ACPD is the marine area adjacent to the North China Plain (Fig. 1), where outflow of large amounts of O_3 precursors could take place during monsoon seasons with prevailing westerly winds (Zhang *et al.*, 2002). As for the northwest region to the study site, it covers one of the most polluted provinces of China (i.e., Jiangsu) with large amounts of O_3 precursors being emitted annually (Li *et al.*, 2016a; Wu *et al.*, 2016). Long-range transported air pollutants from these two regions had probably contributed to the increase in O_3 levels in the study area. The relatively high O_3 concentrations (> 45 ppb) associated with strong north winds during nighttime (Fig. 6(c)) could also confirm this influence of regional transport. Given the large contribution of pollutant transport from other regions to the O_3 pollution in Zhejiang, the coordinated inter-regional control on pollutant emissions in the northern upwind areas will be quite necessary to help improving local and regional air quality.

In addition to the analyses concerning the whole study period, all the pollution episodes with O_3 concentrations continuously exceeding the 75th percentile (51.8 ppb) of the dataset for 8 hours were also analyzed using polarplot technique. Higher O_3 concentrations were experienced with northwest winds when their speeds were higher than 6 m s^{-1} (Fig. 7(a)). This further confirmed the influence of long-range transported pollutants from northwest region (e.g., Jiangsu Province) on surface O_3 at the study site. In terms of the differences between the diurnal and nocturnal O_3 concentrations, all the high O_3 values (> 75 ppb of Grade I NAAQS) were observed during the daylight hours (Fig. 7(b)),

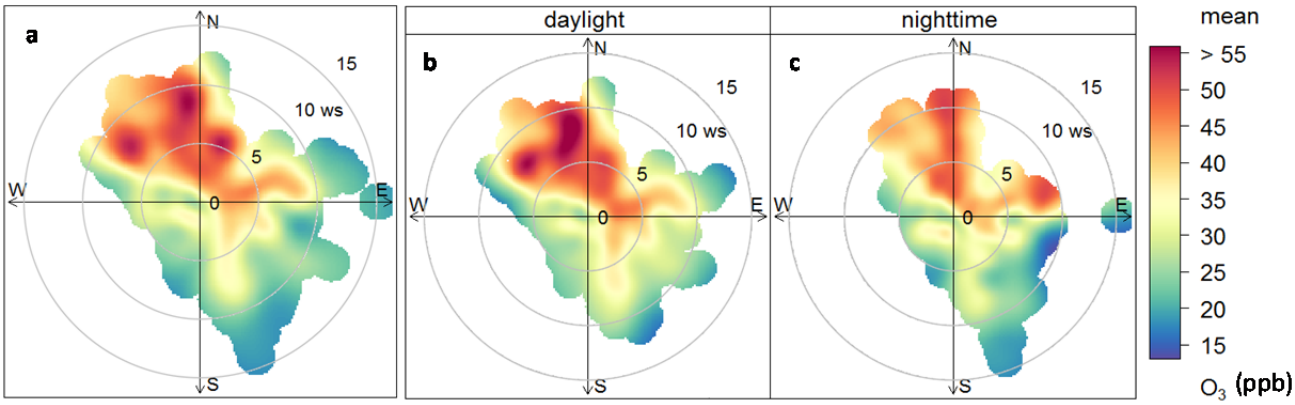

Fig. 6. Polar plots of average O_3 concentrations for the (a) whole day, (b) daytime, and (c) nighttime over the period of June 2013–October 2016 at ACPD.

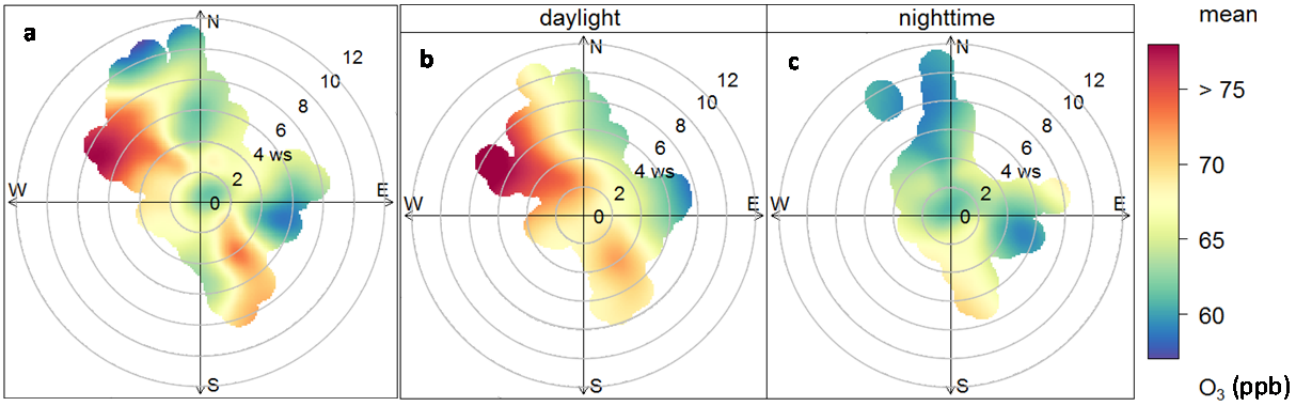

Fig. 7. Polar plots of average O_3 concentrations during the pollution episodes for the (a) whole day, (b) daytime, and (c) nighttime over the period of June 2013–October 2016 at ACPD.

which suggested the critical role of photochemical activities on the O_3 pollution. However, the surface O_3 photochemically produced during the daytime could also accumulate at night, as indicated by the relatively high O_3 levels (50–70 ppb) during the nighttime of the pollution episodes (Fig. 7(c)). Similar nighttime accumulation of O_3 has also been reported in the coastal cities of Europe (e.g., Barcelona, Spain), where the O_3 transport from inland regions was influential (Valverde *et al.*, 2016).

Besides northwest, another transport direction of O_3 during the pollution episodes was also detected to be the southeast when wind speeds were in the range of 2–6 m s^{-1} (Figs. 7(a) and 7(b)). As the southeast region to the study area is in the East China Sea without large emission sources, the air pollutants transported from this direction were probably associated with the human activities (e.g., tourism and freight transportation) on the small islands surrounding ACPD (Fig. 1). It is worth mentioning that a civil airport and an international cruise terminal are located on the island to the southeast of ACPD with distances of 5.5 km and 8.8 km, respectively. The air pollutants emitted from the aircrafts and ships might contribute comprehensively to the O_3 increase in the study area when southeast winds prevailed over Zhoushan. More measurements on precursor emissions from these transportation vehicles are still needed in the future work to confirm this speculation. In contrast to the influence from short-distance transport of air pollutants, local contribution to O_3 pollution is relatively weak as indicated by the low O_3 concentrations at low wind speeds (Figs. 7(a) and 7(b)). This is probably due to the few emission sources of O_3 precursors at the study site as well as the good dispersive conditions of atmosphere.

Potential Areas Contributing to Surface O_3

Based on the PSCF analysis, the major potential areas contributing to surface O_3 at ACPD (weighted PSCF > 0.4) were found to lie in the coastal region of the North China Plain and its adjacent marine areas (Fig. 8). All of them were located to the north and northwest of the study site, which is consistent with the results derived from the polarplot analyses discussed in previous section. The core areas with high probabilities (weighted PSCF > 0.5) were far away (> 400 km) from ACPD, which indicated the contribution of long-range transported pollutants to the O_3 at the study site. The regions to the west and southwest of ACPD (e.g., Zhejiang and Fujian Provinces) are unlikely to be the major potential source areas of O_3, which can be indicated from the relatively low values (< 0.4) of weighted PSCF. Besides the coastal areas of the North China Plain, South Korea was identified as another major O_3 source

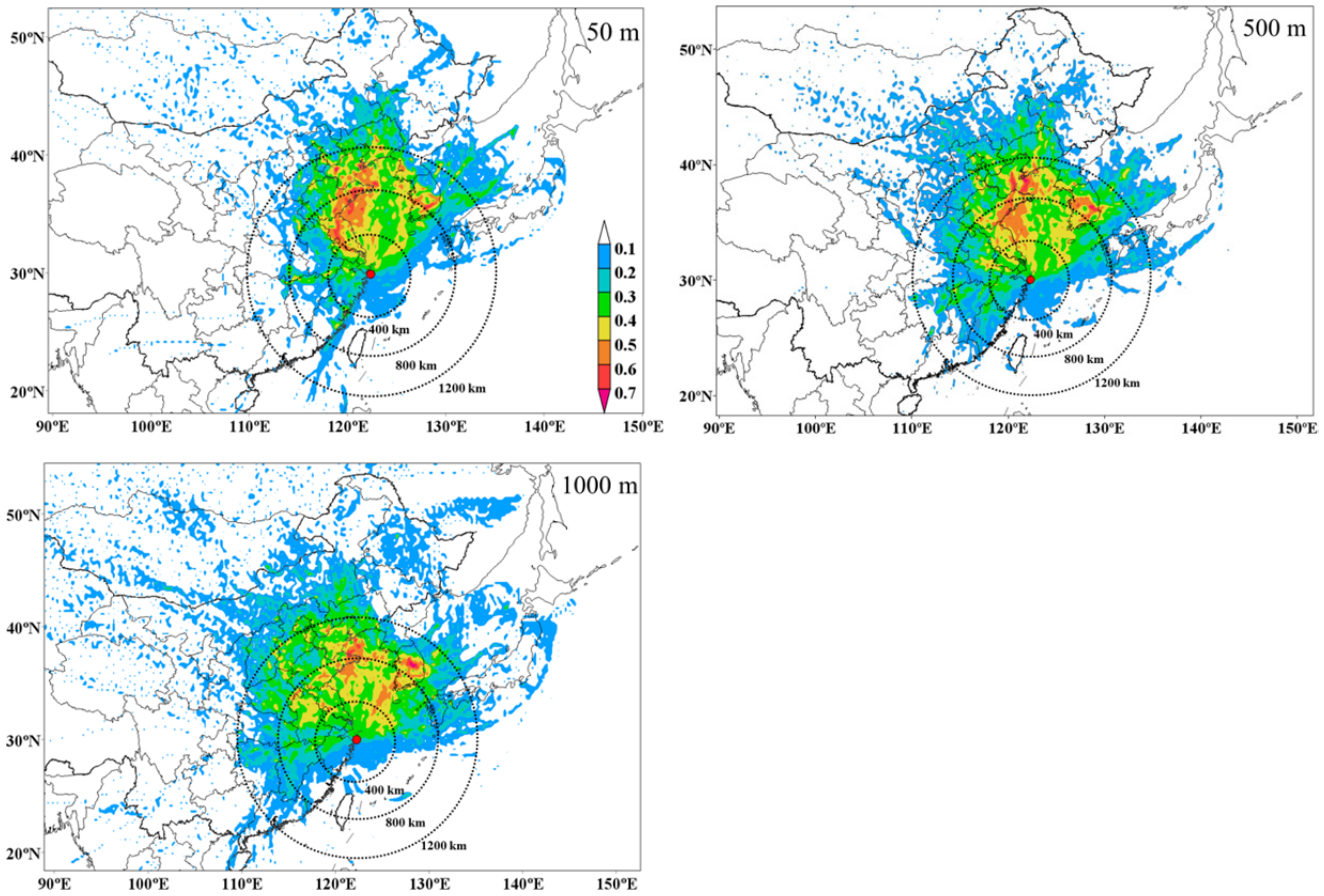

Fig. 8. PSCF maps of the O_3 concentrations greater than 75th percentile value (51.8 ppb) from June 2013 to October 2016 at ACPD with trajectory heights of 50, 500 and 1000 m. The dashed circle lines indicate the distances (400, 800 and 1200 km) from ACPD.

region of ACPD (weighted PSCF > 0.5) (Fig. 8). It is independent from the source region near the North China Plain, and is also far away (> 600 km) from the study site. As a developed Asian country, South Korea is famous for its advanced manufacturing industries (e.g., steel production, automobile manufacturing and shipbuilding). Large amounts of precursors (e.g., NO_2; Fig. S2) are emitted into the atmosphere annually in South Korea (Han *et al.*, 2009; Mijling *et al.*, 2015), which might significantly contribute to the O_3 rise at ACPD via long-range transport.

Trajectory Analyses for the Inflowing Airmasses to Zhejiang Province

During the study period between June 2013 and October 2016, a total of 562 trajectories (44.9%) were identified as the inflowing ones. All these trajectories spent less than three hours in Zhejiang Province, which was determined visually from the endpoints of airmass trajectories. The O_3 data were available on 485 days of the inflowing days with 77 days of them being missing due to the power failure or instrument malfunction.

During the four O_3 seasons over 2013–2016, a total of 70 hourly O_3 concentrations (14:00 CST) greater than NAAQS Grade I (75 ppb) were observed. While under the inflow conditions at 14:00 CST, 45 observations of hourly O_3 exceeded 75 ppb, which accounted for 64.3% of the total exceedances over 75 ppb. This suggested that the O_3 pollution in the study area was predominantly contributed from external transport. As Zhoushan was a border city of Zhejiang Province, the O_3 concentrations in airmasses flowing into this city could represent the background levels in Zhejiang. The obvious O_3 inflow observed at ACPD indicated a high contribution of regional transport to surface O_3 in Zhejiang, especially for the cities close to Zhoushan. In order to meet the O_3 requirements of NAAQS in Zhejiang Province, the coordinated inter-regional prevention and control on pollutant emissions should be carried out.

For the purpose of identifying the major pathways of O_3 transported into Zhejiang Province via the study area, cluster analysis was made using the 485 inflowing trajectories. Four trajectory clusters were derived with two representing the airmasses from East China Sea (Clusters 1 and 4), and two representing the ones from the coastal region of the North China Plain (Clusters 2 and 3) (Fig. 9). The frequencies of airmass trajectories varied from 9.8% (Cluster 4) to 36.5% (Cluster 2), with more than half (53.7%) of them coming from north to the study area (Table 2). In terms of the average O_3 concentrations for different clusters, high levels (> 56.0 ppb) were observed

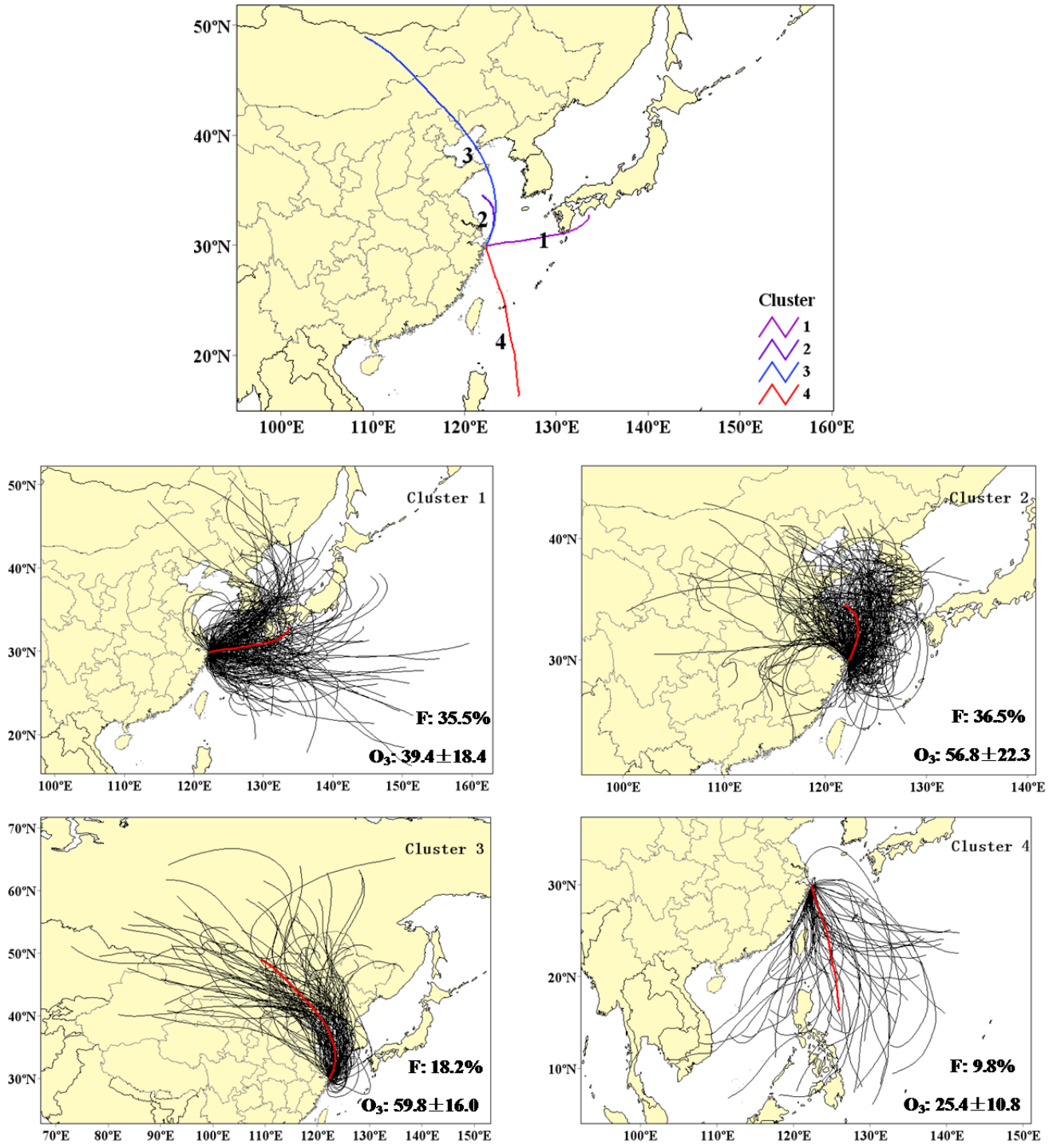

Fig. 9. Mean backward trajectory clusters and the trajectories associated with each cluster from June 2013 to October 2016 at ACPD.

Table 2. Statistics of the O_3 levels for the four trajectory clusters.

Cluster	Number	Frequency (%)	Avg. ± Std (ppb)	Median (ppb)	75th percentile (ppb)	Max. O_3 (ppb)	Ratio[a] (%)
1	200	35.5	39.4 ± 18.4	39.2	51.3	102.2	9.0
2	205	36.5	56.8 ± 22.3	55.3	67.9	154.0	32.7
3	102	18.2	59.8 ± 16	57.9	67.0	109.7	34.3
4	55	9.8	25.4 ± 10.8	23.8	31.5	54.6	0.0

[a] Ratio represents the percentage of O_3 level over 75th percentile which is 51.8 ppb.

for the airmasses from the north region to the study site (Clusters 2 and 3) (Table 2 and Fig. 10(a)). The percentages of O_3 levels greater than the 75th percentile (51.8 ppb) were also high (> 30%) for Clusters 2 and 3. Both the high frequencies and high O_3 levels for the northern clusters (2 and 3) indicated that the coastal area of the North China Plain was the major potential region contributing to the O_3 pollution in Zhejiang Province. This is consistent with the results derived from the polarplot and PSCF analyses in this study. In contrast, the O_3 concentrations in the airmasses coming from the southeast marine area (Cluster 4) were the lowest (avg.: 25.4 ppb), with no O_3 values over the 75th percentile (51.8 ppb) being observed. The lack of emission sources of O_3 precursors in the southeast marine area could account for the relatively low O_3 levels for the airmasses from this direction.

As to the "polluted" northern clusters (2 and 3), the O_3 concentrations for Cluster 3 (avg.: 59.8 ppb) were significantly higher ($p = 0.032$) than those of Cluster 2 (avg.: 56.8 ppb) (Table 2). In comparison with the airmasses of Cluster 2, those of Cluster 3 had longer transport pathways through the whole Hebei Province (Fig. 9), which is one of the most polluted regions of China (Wang *et al.*, 2013). This suggested that the airmasses associated with Cluster 3 might carry more O_3 precursors than those of Cluster 2, which could lead to the higher levels of O_3 via photochemical reactions during transport. Besides, O_3 concentration is usually negatively correlated with relative humidity due to the O_3 removal through reactions with water vapor (Fiore *et al.*, 2002). In this study, a significant negative correlation between O_3 concentration and relative humidity was observed for the inflowing airmasses ($r = –0.58$, $p < 0.001$). Cluster 3 was characterized by the lowest relative humidity of the four clusters (Fig. 10(d)), which was more suitable for the accumulation of O_3. Therefore, higher O_3 concentrations were observed for the airmasses represented by Cluster 3. In addition to the relationship between O_3 and relative humidity, it is also worth noting that the O_3 concentration had an opposite trend of variation to that of air temperature among the four clusters (Fig. 10), with the highest O_3 level but the lowest temperature being observed for Cluster 3. This was similar to the result observed in the monthly variations of O_3 and air temperature (Figs. 3 and 4). The city of Zhoushan has a typical subtropical climate with airmasses from northwest inland of China being prevalent in cold seasons. Therefore, low air temperature was more associated with the northwest airmasses (represented by Clusters 2 and 3), which could carry a considerable amount of precursor pollutants (e.g., VOCs) emitted from northern China (Wu *et al.*, 2016). This might account for the opposite trends between O_3 and air temperature among clusters (Fig. 10).

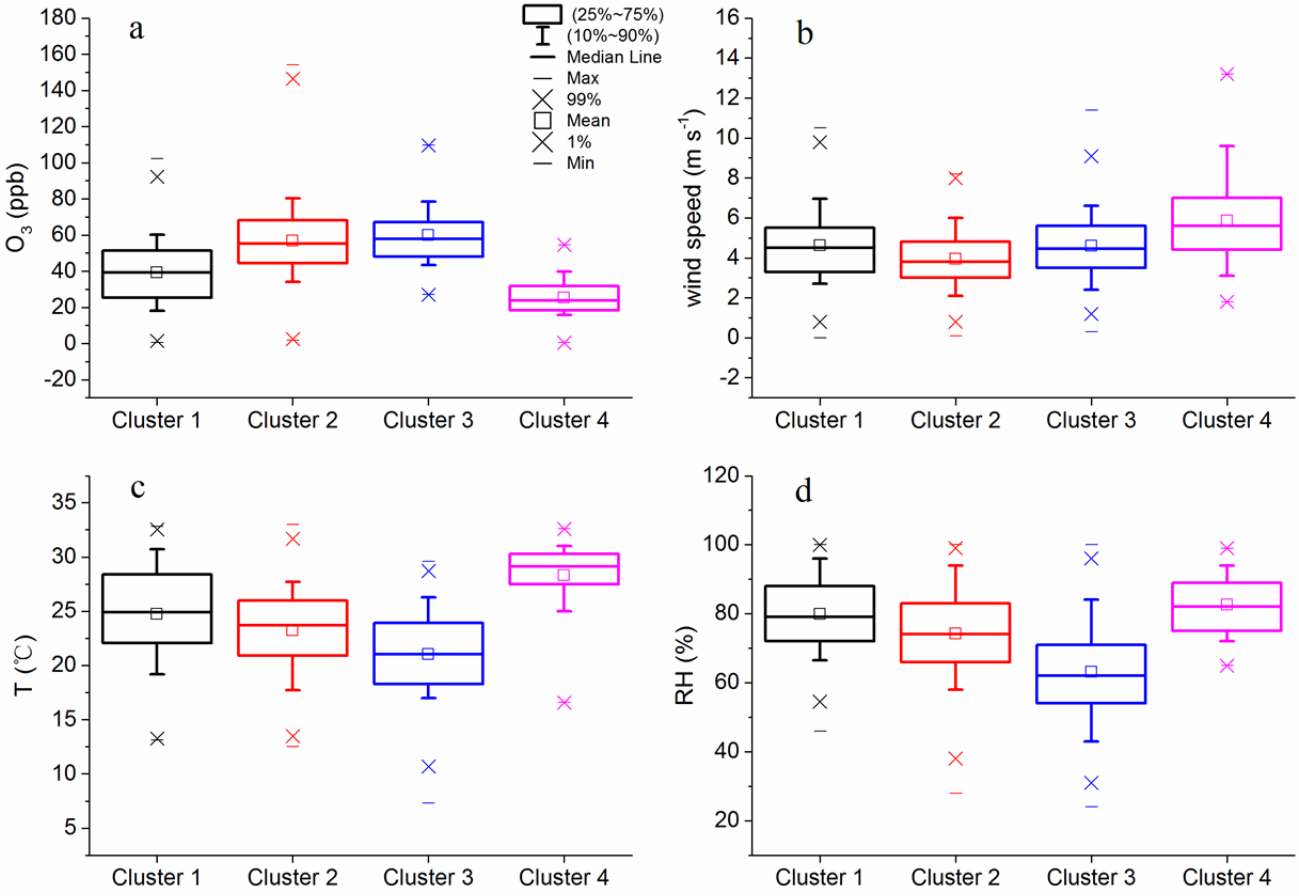

Fig. 10. Box plots of (a) O_3 concentration, (b) wind speed, (c) air temperature, and (d) relative humidity at ACPD for the four trajectory clusters.

Ozone Episode Analyses

In order to further identify the potential regions contributing to surface O_3 over the study area, typical episodes with obvious changes in wind directions were selected based on the following rules. Firstly, the days with hourly O_3 levels exceeding 75th percentile (51.8 ppb) of the dataset for at least three consecutive hours (Period I) were selected. Secondly, the days with obvious and continuous changes in hourly wind directions (Period II) were selected. Thirdly, the intersection between Periods I and II was selected as the days of episodes. The O_3 concentrations in these episodes were analyzed along with wind speeds, air temperature, relative humidity, rainfall, and the 72-h back trajectories of airmasses with the arrival time at ACPD of 14:00 (CST), when the O_3 concentrations were relatively high. Besides, the O_3 levels in the neighboring provinces of Zhoushan (Fig. S2), where the back trajectories had passed through, were also analyzed to preliminarily explore the possible contributing mechanisms of external sources to local O_3 in the study area.

Case Study 1

Obvious variations in O_3 concentrations and meteorological variables including wind direction, wind speed, air temperature and relative humidity were observed from June 3 to June 8, 2014 (Fig. 11). The wind direction changed suddenly from northwest to southeast in the middle of this period. Before June 6, high O_3 concentrations were observed under relatively cold and dry weather conditions which were associated with strong northwest winds. This is especially obvious on June 3 and June 4, when the maximum hourly O_3 and wind speed reached as high as 90 ppb and 7 m s^{-1}, respectively. The O_3 concentration varied positively with wind speed before June 6 with the maximum values of both variables occurring almost simultaneously. This indicated that the regional transport of air pollutants had significantly contributed to the O_3 rise at the study site. Based on the back trajectory analyses, the airmasses to ACPD on June 3 and June 4 (14:00 CST) were found to pass through Shandong Peninsula, Jiangsu Province and Shanghai Municipality (Fig. S4), where large emissions of O_3 precursors (Li *et al.*, 2016a; Wu *et al.*, 2016) had probably contributed to the high levels of O_3 observed in the study area. As the airmasses were mainly in Jiangsu Province within 24 hours before arriving at the study site on June 3 and June 4 (Fig. S4), the O_3 levels in 13 cities of Jiangsu as well as Shanghai (Fig. S2) from June 2 to June 3 were analyzed on the regional basis (Fig. S5). The regional average O_3 levels varied from 23.5 to 55.1 ppb during the period of June 2–3, with the maximum hourly average O_3 concentration of 80.1 ppb being observed in the city of Xuzhou (XZ). This indicated that the direct pollutant transport from upwind cities in Jiangsu Province could contribute a considerable amount of O_3 to the study area. However, it is noteworthy that the O_3 levels at the study site were generally higher than those of the 14 upwind cities. This might be accounted for by the following two reasons. Firstly, most of the state controlled stations used for the O_3 analyses of the 14 cities are located in or near urban areas (http://datacenter.mep.gov.cn/), where the O_3 levels were usually lower than those in non-urban areas due to the titration of NO from traffic emissions (Londhe *et al.*, 2008). Therefore, the average O_3 levels in the whole region of Jiangsu should be higher than the values calculated in this study, and closer to the levels at the study site. Secondly, offshore regions are important areas for O_3 formation due to the large supply of

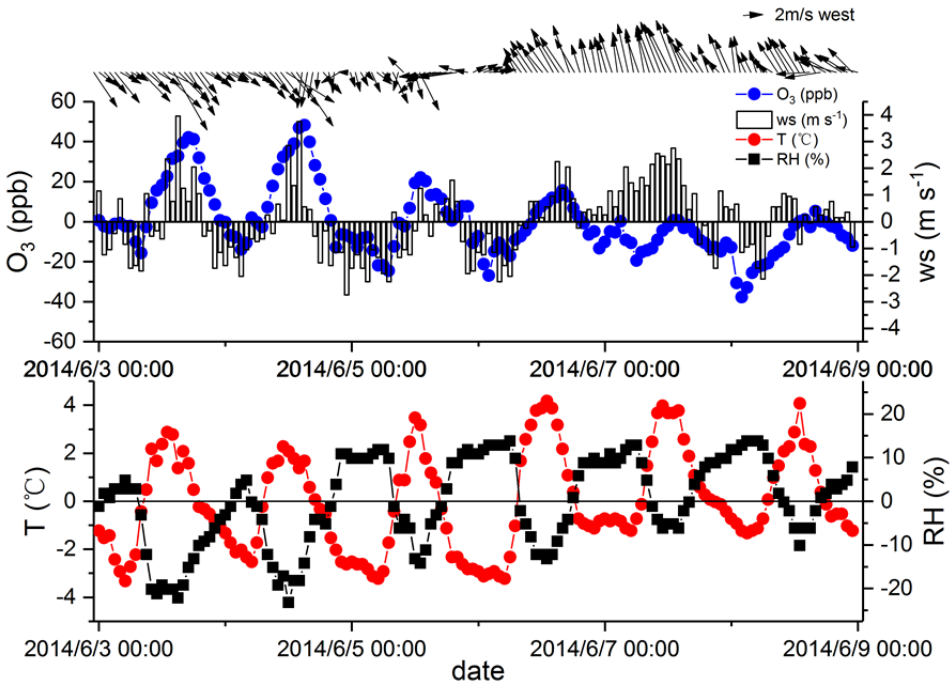

Fig. 11. Plots of anomalies from the period averages for the hourly O_3 concentration, wind direction, wind speed, air temperature, and relative humidity at ACPD from June 3 to June 8, 2014.

precursors from mainland cities (Zhang *et al.*, 2002) and suitable photochemical conditions (e.g., high levels of chlorine radical) (Knipping and Dabdub, 2003). More O_3 might be produced in the lower marine atmosphere before the airmasses arriving at Zhoushan Islands, and finally resulted in the higher levels of O_3 at the study site. More studies based on long-term monitoring in the rural and marine areas along the transport pathways are still needed to confirm these assumptions in our future work.

Compared to the high levels of O_3 on June 3 and June 4, much lower values were observed on June 7 and June 8, when the relatively strong southeast winds (4.4 m s^{-1} on diurnal average) could significantly affect local air quality of Zhoushan (Fig. 11). As the airmasses arriving at Zhoushan on June 7 and June 8 mainly came from East China Sea (Fig. S4), the obvious decrease in O_3 levels during this episode was probably caused by the diluting effect of the clean and humid airmasses from the marine area. Based on the comparative analyses of O_3 levels during the period of June 3–8, the major potential region contributing to surface O_3 over Zhoushan was found to lie to the northwest of the study area, while the southeast marine area was probably a clean region with lower levels of O_3 in the atmosphere. This further confirmed the inferences on the potential source regions of O_3 in Zhoushan made in previous sections.

Case Study 2

During the period from May 9 to May 10, 2016, significant increases in O_3 levels and wind speeds occurred along with obvious changes in wind directions from east to northwest (Fig. 12). In this episode, the study site was under the influence of cyclone systems (Fig. S6), which are usually associated with cloudy and rainy weather conditions. The air temperature was relatively low, especially on May 10 when the cold and dry airmasses from northwest prevailed over the site (Fig. 12). It began to rain at late night of May 9 and lasted to the morning of May 10. These weather conditions indicated weak photochemical activities, which are not suitable for local O_3 formation. Given the relatively high levels of daily O_3 occurred under high wind speeds on both May 9 and May 10, surface O_3 at the study site was regarded to be largely contributed from external transport.

In the afternoon (14:00) of May 9, the airmass arriving at ACPD mainly passed through the coastal provinces of Southeast China (Fig. S7). The relatively low O_3 concentrations (avg.: 35.0 ppb) observed in the daytime of May 9 indicated the upwind provinces (e.g., Fujian and Zhejiang) in Southeast China contributed less O_3 to the study area. This can be confirmed by the lower O_3 levels in Fujian Province (6.9–33.2 ppb) and southeast Zhejiang Province (7.7–30.2 ppb) within 24 hours before the airmass arriving at the study site (Figs. S8(a) and 8(b)). Compared with the diurnal average O_3 concentration on May 9 (35.0 ppb), the value was obviously higher on May 10 (51.8 ppb), when the airmass came from northwest to the study area (i.e., Jiangsu Province and Shanghai Municipality) (Fig. S7). The average O_3 concentrations in this region varied from 13.8 to 57.2 ppb, with the peak values over 60 ppb in the southern part of Jiangsu Province (e.g., WX and CZ) (Fig. S8(c)). This indicated significant contribution of O_3 from Jiangsu to the study area. Based on the analyses of this episode from May 9 to May 10, 2016, the major potential areas contributing to the O_3 at ACPD were found to lie in the region northwest to Zhoushan (e.g., Jiangsu),

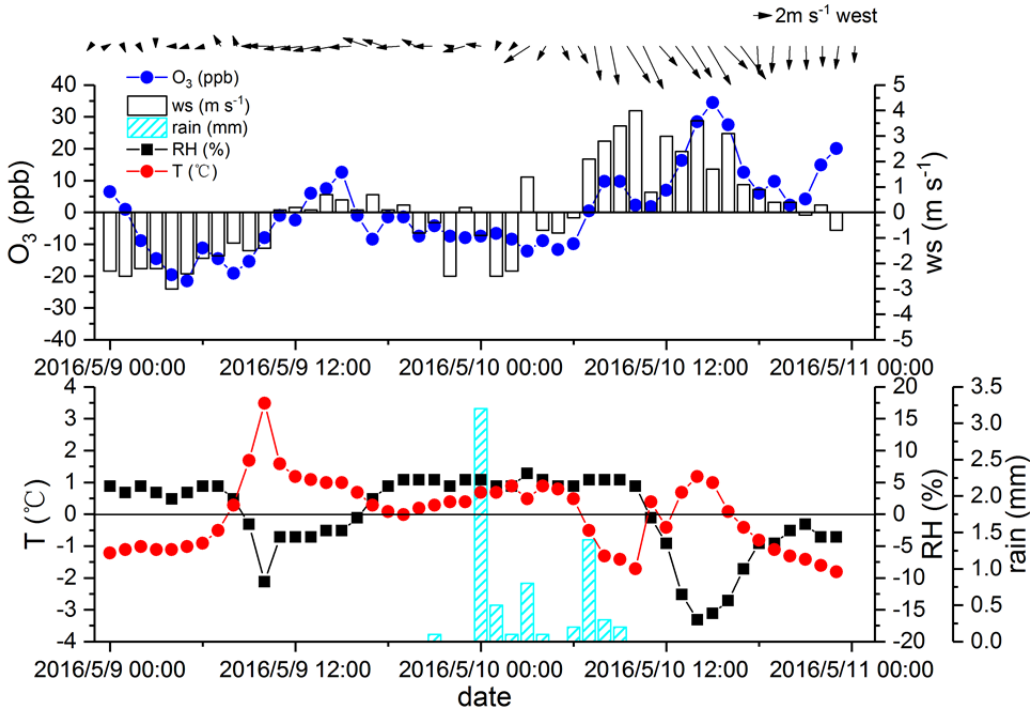

Fig. 12. Plots of anomalies from the period averages for the hourly O_3 concentration, wind direction, wind speed, air temperature, relative humidity, and the hourly variation of rainfall at ACPD from May 9 to May 10, 2016.

while the southeast provinces (e.g., Fujian) were more likely to be a clean source region with low O_3 concentrations.

CONCLUSIONS

With surface concentrations frequently exceeding the NAAQS of China, the O_3 pollution is serious in the city of Zhoushan, posing high potential health risks to locals. Opposite trends of monthly variations were observed for the O_3 and air temperature, with obviously decreased O_3 occurring in summer, probably due to the influence of intense rainfall, high relative humidity and clean marine airmasses during this season. The transport of external air pollutants has played a dominant role in the rise of surface O_3 at this coastal site in eastern China, which is comprehensively indicated by the high O_3 concentrations (> 50 ppb) under high wind speeds (> 5 m s^{-1}) from the north and northwest, the time lag for the occurrence of the maximum daily O_3 concentrations, and the high incidence (64.3%) of O_3 pollution under inflow conditions.

Although the coastal regions of China have been developed, the contributions of pollutants from these areas to the surface O_3 in Zhoushan clearly varied. Based on the source identification, the major regions contributing to the surface O_3 at ACPD were found to lie to the north and northwest of the study area. Long-range transported air pollutants from the coastal provinces of the North China Plain (e.g., Shandong and Jiangsu) as well as South Korea may have significantly increased the surface O_3 at the study site, while the coastal provinces to the southwest of the study area (e.g., Fujian) are relatively clean and produced less O_3 output to Zhoushan. In contrast to the contribution from regional transport, the local contribution to the surface O_3 was small, with much lower O_3 concentrations being observed under low wind speeds.

Significant background transport of O_3 to Zhejiang was confirmed, with nearly two thirds of the pollution episodes at ACPD being accounted for by the airmasses originating outside Zhejiang. This is especially true for the airmasses coming from north of the study area, with high levels (> 56.0 ppb) of O_3 being observed for the northern trajectory clusters. In order to meet the NAAQS on O_3 in the whole province of Zhejiang, the influx of pollutants from the coastal region of northern China must be reduced, which will require coordinated inter-regional control on pollutant emissions in the northern upwind areas.

ACKNOWLEDGMENTS

We thank the anonymous reviewers for their helpful comments and suggestions. The research was supported by the National Natural Science Foundation of China (Nos. 31300435, U1405235), Science and Technology Plan Project of Ningbo City (No. 2015C110001), and Natural Science Foundation of Ningbo City (No. 2017A610295).

SUPPLEMENTARY MATERIAL

Supplementary data associated with this article can be found in the online version at http://www.aaqr.org.

REFERENCES

Aleksic, N., Kent, J. and Walcek, C. (2016). Ozone concentrations in air flowing into New York State. *Atmos. Environ.* 141: 454–461.

Ashbaugh, L.L., Malm, W.C. and Sadeh, W.Z. (1985). A residence time probability analysis of sulfur concentrations at grand Canyon National Park. *Atmos. Environ.* 19: 1263–1270.

Berntsen, T.K., Karlsdottir, S. and Jaffe, D.A. (1999). Influence of Asian emissions on the composition of air reaching the north western United States. *Geophys. Res. Lett.* 26: 2171–2174.

Carslaw, D.C., Beevers, S.D., Ropkins, K. and Bell, M.C. (2006). Detecting and quantifying aircraft and other on-airport contributions to ambient nitrogen oxides in the vicinity of a large international airport. *Atmos. Environ.* 40: 5424–5434.

Chiang, C.K., Fan, J.F., Li, J. and Chang, J.S. (2009). Impact of Asian continental outflow on the springtime ozone mixing ratio in northern Taiwan. *J. Geophys. Res.* 114: D24304.

Demuzere, M., Trigo, R.M., Arellano, V.G.D. and Lipzig, N.P.M.V. (2009). The impact of weather and atmospheric circulation on O_3 and PM_{10} levels at a mid-latitude site. *Atmos. Chem. Phys.* 9: 2695–2714.

Draxler, R.R., Stander, B., Rolph, G., Stein, A. and Taylor, A. (2014). *HYSPLIT4 user's guide (Version 4)*. NOAA Technical Memorandum ERL ARL.

Dueñas, C., Fernández, M.C., Cañete, S. Carretero, J. and Liger, E. (2004). Analyses of ozone in urban and rural sites in Malaga (Spain). *Chemosphere* 56: 631–639.

Fann, N., Lamson, A.D., Anenberg, S.C., Wesson, K., Risley, D. and Hubbell, B.J. (2012). Estimating the national public health burden associated with exposure to ambient $PM_{2.5}$ and ozone. *Risk Anal.* 32: 81–95.

Feng, Z., Hu, E., Wang, X., Jiang, L. and Liu, X. (2015). Ground-level O_3 pollution and its impacts on food crops in China: A review. *Environ. Pollut.* 199: 42–48.

Fiore, A.M., Jacob, D.J., Bey, I., Yantosca, R.M., Field, B.D., Fusco, A.C. and Wilkinson, J.G. (2002). Background ozone over the United States in summer: Origin, trend, and contribution to pollution episodes. *J. Geophys. Res.* 107: ACH 11-11–ACH 11-25.

Fu, X., Wang, S., Zhao, B., Xing, J., Cheng, Z., Liu, H. and Hao, J. (2013). Emission inventory of primary pollutants and chemical speciation in 2010 for the Yangtze River Delta region, China. *Atmos. Environ.* 70: 39–50.

Gonçalves, M., Jiménez-Guerrero, P. and Baldasano, J.M. (2009). Contribution of atmospheric processes affecting the dynamics of air pollution in south-western Europe during a typical summertime photochemical episode. *Atmos. Chem. Phys.* 9: 849–864.

Grange, S.K., Lewis, A.C. and Carslaw, D.C. (2016). Source apportionment advances using polar plots of bivariate correlation and regression statistics. *Atmos.*

Environ. 145: 128–134.

Han, K.M., Song, C.H., Ahn, H.J., Park, R.S., Woo, J.H., Lee, C.K., Richter, A., Burrows, J.P., Kim, J.Y. and Hong, J.H. (2009). Investigation of NO_x emissions and NO_x- related chemistry in East Asia using CMAQ-predicted and GOME-derived NO_2 columns. *Atmos. Chem. Phys.* 9: 1017–1036.

Jo, W.K. and Park, J.H. (2005). Characteristics of roadside air pollution in Korean metropolitan city (Daegu) over last 5 to 6 years: Temporal variations, standard 0s. *Chemosphere* 59: 1557–1573.

Kanaya, Y., Tanimoto, H., Yokouchi, Y., Taketani, F., Komazaki, Y., Irie, H., Takashima, H., Pan, X., Nozoe, S. and Inomata, S. (2016). Diagnosis of photochemical ozone production rates and limiting factors in continental outflow air masses reaching Fukue Island, Japan: Ozone-control implications. *Aerosol Air Qual. Res.* 16: 430–441.

Knipping, E.M. and Dabdub, D. (2003). Impact of chlorine emissions from sea-salt aerosol on coastal urban ozone. *Environ. Sci. Technol.* 37: 275–284.

Li, K., Chen, L., Ying, F., White, S.J., Jang, C., Wu, X., Gao, X., Hong, S., Shen, J., Azzi, M. and Cen, K. (2017). Meteorological and chemical impacts on ozone formation: A case study in Hangzhou, China. *Atmos. Res.* 196: 40–52.

Li, L., An, J.Y., Shi, Y.Y., Zhou, M., Yan, R.S., Huang, C., Wang, H.L., Lou, S.R., Wang, Q., Lu, Q. and Wu, J. (2016a). Source apportionment of surface ozone in the Yangtze River Delta, China in the summer of 2013. *Atmos. Environ.* 144: 194–207.

Li, Y., Ye, C., Liu, J., Zhu, Y., Wang, J., Tan, Z., Lin, W., Zeng, L. and Zhu, T. (2016b). Observation of regional air pollutant transport between the megacity Beijing and the North China Plain. *Atmos. Chem. Phys.* 16: 14265–14283.

Lin, M., Fiore, A.M., Horowitz, L.W., Langford, A.O., Oltmans, S.J., Tarasick, D. and Rieder, H.E. (2015). Climate variability modulates western US ozone air quality in spring via deep stratospheric intrusions. *Nat. Commun.* 6: 7105.

Londhe, A.L., Jadhav, D.B., Buchunde, P.S. and Kartha, M.J. (2008). Surface ozone variability at urban and nearby rural locations of tropical India. *Curr. Sci.* 95: 1724–1729.

Ma, J.Z., Zhou, X.J. and Hauglustaine, D. (2002). Summertime tropospheric ozone over china simulated with a regional chemical transport model. 2. Source contributions and budget. *J. Geophys. Res.* 107: 4612.

Mavroidis, I. and Ilia, M. (2012). Trends of NO_x, NO_2, and O_3, concentrations at three different types of air quality monitoring stations in Athens, Greece. *Atmos. Environ.* 63: 135–147.

Mijling, B., Johannes, V.D.A.R., Ding, J.Y. and Stavrakou, J. (2015). Emission estimates for India and East Asia. User Consultation Meeting, Doha, Qatar, 24–25 Nov. 2015.

Monks, P.S., Archibald, A.T., Colette, A., Cooper, O., Coyle, M., Derwent, R., Fowler, D., Granier, C., Law, K.S., Mills, G.E., Stevenson, D.S., Tarasova, O., Thouret, V., von Schneidemesser, E., Sommariva, R., Wild, O. and Williams, M.L. (2015). Tropospheric ozone and its precursors from the urban to the global scale from air quality to short-lived climate forcer. *Atmos. Chem. Phys.* 15: 8889–8973.

Nopmongcol, U., Jung, J., Kumar, N. and Yarwood, G. (2016). Changes in US background ozone due to global anthropogenic emissions from 1970 to 2020. *Atmos. Environ.* 140: 446–455.

Ou, J., Yuan, Z., Zheng, J., Huang, Z., Shao, M., Li, Z., Huang, X., Guo, H. and Louie, P.K.K. (2016). Ambient ozone control in a photochemically active region: Short term despiking or long-term attainment? *Environ. Sci. Technol.* 50: 5720–5728.

Pope, R.J., Butt, E.W., Chipperfield, M.P., Doherty, R.M., Fenech, S., Schmidt, A., Arnold, S.R. and Savage, N.H. (2016). The impact of synoptic weather on UK surface ozone and implications for premature mortality. *Environ. Res. Lett.* 11: 124004.

Reddy, B.S.K., Kumar, K.R., Balakrishnaiah, G., Gopal, K.R., Reddy, R., Sivakumar, V., Lingaswamy, A., Arafath, S.M., Umadevi, K. and Kumari, S.P. (2012). Analysis of diurnal and seasonal behavior of surface ozone and its precursors (NO_x) at a semi-arid rural site in southern India. *Aerosol Air Qual. Res.* 12: 1081–1094.

Shen, L., Mickley, L.J. and Tai, A.P.K. (2015). Influence of synoptic patterns on surface ozone variability over the eastern United States from 1980 to 2012. *Atmos. Chem. Phys.* 15: 13073–13108.

Sillman, S. (1999). The relation between ozone, NO_x and hydrocarbons in urban and polluted rural environments. *Atmos. Environ.* 33: 1821–1845.

Stocker, T.F., Qin, D., Plattner, G.K., Tignor, M.M.B., Allen, S.K., Boschung, J., Nauels, A., Xia, Y., Bex, V. and Midgley, P.M. (2013). IPCC: Climate Change 2013: The assessment reports of the intergovernmental panel on climate change. Cambridge University Press, Cambridge, UK, pp. 1552.

Sudo, K. and Akimoto, H. (2007). Global source attribution of tropospheric ozone: Long-range transport from various source regions. *J. Geophys. Res.* 112: D12302.

Thermo Fisher Scientific Inc. (2017). *Model 49i Instruction Manual*, Franklin, Massachusetts, USA.

Tong, L., Zhang, H., Yu, J., He, M., Xu, N., Zhang, J., Qian, F., Feng, J. and Xiao, H. (2017a). Characteristics of surface ozone and nitrogen oxides at urban, suburban and rural sites in Ningbo, China. *Atmos. Res.* 187: 57–68.

Tong, L., Zhang, J.J., Xiao, H., Cai, Q.L., Huang, Z.W., Zhang, H.L., Zheng, J., He, M.M., Peng, C.H., Feng, J.Y. and Qian, F.Z. (2017b). Identification of the potential regions contributing to ozone at a coastal site of eastern China with air mass typology. *Atmos. Pollut. Res.* 8: 1044–1057.

Valverde, V., Pay, M.T. and Baldasano, J.M. (2016). Ozone attributed to Madrid and Barcelona on-road transport emissions: Characterization of plume dynamics over the Iberian Peninsula. *Sci. Total Environ.* 543: 670–682.

Vellingiri, K., Kim, K.H., Lim, J.M., Lee, J.H., Ma, C.J., Jeon, B.H., Sohn, J.R., Kumar, P. and Kang, C.H. (2016). Identification of nitrogen dioxide and ozone source regions for an urban area in Korea using back trajectory analysis. *Atmos. Res.* 176: 212–221.

Vingarzan, R. (2004). A review of surface ozone background levels and trends. *Atmos. Environ.* 38: 3431–3442.

Wang, H., Zhou, L. and Tang, X. (2006). Ozone concentrations in rural regions of the Yangtze Delta in China. *J. Atmos. Chem.* 54: 255–265.

Wang, L., Liu, Z., Sun, Y., Ji, D. and Wang, Y. (2015). Long-range transport and regional sources of $PM_{2.5}$ in Beijing based on long-term observations from 2005 to 2010. *Atmos. Res.* 157: 37–48.

Wang, L., Yang, J., Zhang, P., Zhao, X., Wei, Z., Zhang, F., Su, J. and Meng, C. (2013). A review of air pollution and control in Hebei Province, China. *Open J. Air Pollut.* 2: 47–55.

Wang, Y.Q., Zhang, X.Y. and Draxler, R.R. (2009). TrajStat: GIS-based software that uses various trajectory statistical analysis methods to identify potential sources from long-term air pollution measurement data. *Environ. Modell. Software* 24: 938–939.

Wu, R.R., Bo, Y., Li, J., Li, L.Y., Li, Y.Q. and Xie, S.D. (2016). Method to establish the emission inventory of anthropogenic volatile organic compounds in China and its application in the period 2008–2012. *Atmos. Environ.* 127: 244–254.

Xu, J., Ma, J.Z., Zhang, X.L., Xu, X.B., Xu, X.F., Lin, W.L., Wang, Y., Meng, W. and Ma, Z.Q. (2011). Measurements of ozone and its precursors in Beijing during summertime: Impact of urban plumes on ozone pollution in downwind rural areas. *Atmos. Chem. Phys.* 11: 12241–12252.

Xu, X., Lin, W., Wang, T., Yan, P., Tang, J., Meng, Z. and Wang, Y. (2008). Long-term trend of surface ozone at a regional background station in eastern China 1991-2006: Enhanced variability. *Atmos. Chem. Phys.* 8: 2595–2607.

Yu, K.N., Cheung, Y.P., Cheung, T. and Henry, R.C. (2004). Identifying the impact of large urban airports on local air quality by nonparametric regression. *Atmos. Res.* 38: 4501–4507.

Zhang, B.N. and Oanh, N.T.K. (2002). Photochemical smog pollution in the Bangkok Metropolitan Region of Thailand in relation to O_3 precursor concentrations and meteorological conditions. *Atmos. Environ.* 36: 4211–4222.

Zhang, M.G., Uno, I., Sugata, S., Wang, Z.F., Byun, D. and Akimoto, H. (2002). Numerical study of boundary layer ozone transport and photochemical production in East Asia in the wintertime. *Geophys. Res. Lett.* 29: 40-41–40-44.

Zhu, B., Hou, X. and Kang, H. (2016). Analysis of the seasonal ozone budget and the impact of the summer monsoon on the northeastern Qinghai-Tibetan Plateau. *J. Geophys. Res.* 121: 2029–2042.

Received for review, November 17, 2017
Revised, April 23, 2018
Accepted, July 14, 2018